https://doi.org/10.5194/angeo-2021-67
Preprint. Discussion started: 15 December 2021

Annales Geophysicae Discussions

Determination of Tropical Belt Widening Using Multiple GNSS Radio Occultation Measurements

Mohamed Darrag[1,2], Shuanggen Jin[1,3*], Andrés Calabia[1] and Aalaa Samy[2]

[1]School of Remote Sensing and Geomatics Engineering, Nanjing University of Information Science and Technology, Nanjing, China

[2]National Research Institute of Astronomy and Geophysics-NRIAG, 11421- Helwan, Cairo, Egypt

[3]Shanghai Astronomical Observatory, Chinese Academy of Science, Shanghai, China

*Corresponding author: sgjin@nuist.edu.cn; sg.jin@yahoo.com

Abstract

In the last decades, Global navigation satellite systems (GNSS) have provided an exceptional opportunity to retrieve atmospheric parameters globally through GNSS radio occultation (GNSS-RO). In this paper, data of 12 GNSS-RO missions from June 2001 to November 2020 with high resolution were used to investigate the possible widening of the tropical belt along with the probable drivers and impacts in both hemispheres. Applying both lapse rate tropopause (LRT) and cold point tropopause (CPT) definitions, the global tropopause height shows increase of approximately 36 m/decade and 60 m/decade, respectively. Moreover, the tropical edge latitude (TEL) estimated based on two tropopause height metrics, in the northern hemisphere (NH) and southern hemisphere (SH), are different from each other. For the first metric, subjective method, the tropical width from GNSS has expansion behavior in NH with ~ 0.41°/decade and a minor expansion in SH with ~ 0.08°/decade. In case of ECMWF Reanalysis v5 (ERA5) there is no significant contraction in both NH and SH. For Atmospheric Infrared Sounder (AIRS), there are expansion behavior in NH with ~ 0.34°/decade and strong contraction in SH with ~ -0.48°/decade. Using the second metric, objective method, the tropical width from GNSS has expansion in NH with ~ 0.13°/decade, and no significant expansion in SH. In case of ERA5, there is no significant signal in NH while SH has a minor contraction. AIRS has an expansion with ~ 0.13°/decade in NH, and strong contraction in SH with ~ -0.37°/decade. The variability of tropopause parameters (temperature and height) is maximum around the TEL locations at both hemispheres. The total column ozone (TCO) shows increasing rates globally, and the rate of increase at the SH is higher than that of the NH. There is a good agreement between the spatial and temporal patterns of TCO variability and the TEL location estimated from GNSS LRT height. Carbon dioxide (CO_2), and Methane (CH_4), the most important greenhouse gases (GHGs) and the main drivers of global warming, have a global increasing rate and the increasing rate of the NH is similar to that of the SH. The spatial pattern in the NH is located more pole ward than its equivalent at the SH. Both surface temperature and precipitation increase in time and have strong correlation with GNSS LRT height. Both show higher increasing rates at the NH, while the precipitation at the SH has slight decrease and the surface temperature increases. The surface temperature shows a spatial pattern with strong variability, which broadly agrees with the TEL locations. The spatial pattern of precipitation shows northward occurrence. In addition, Standardized Precipitation Evapotranspiration Index (SPEI) has no direct connection with the TEL behavior.

Keywords: GNSS-RO, Tropopause, Tropical belt, climate change.

https://doi.org/10.5194/angeo-2021-67
Preprint. Discussion started: 15 December 2021

1. Introduction

Several studies have reported a widening of the tropics in observations, model simulations and reanalyses. This expansion may lead to profound changes in the global climate system, even a minor expansion of the tropical belt would have significant implications because the shift of the jet streams and subtropical dry zones toward poles have direct effects on weather and precipitation patterns. The widening of the tropical belt is largely considered to be a response to global warming caused by increased GHGs concentrations (Davis and Rosenlof, 2012; Davis and Birner, 2013; Staten et al., 2018; Grise et al., 2019; Watt-Meyer et al., 2019). The reported widening rates range from 0.25° to 2.0° latitude/decade and their statistical significance vary by large amount based on the metrics used to estimate the TEL as well as the data sets utilized for its derivation. In addition, the used metrics may respond in different ways to the force driving the widening because of their differing physics (Davis and Rosenlof, 2012).

In astronomy and cartography, the edges of the tropical belt are the Tropics of Cancer and Capricorn, at latitudes of ~23.5º north and south, where the Sun is directly overhead at solstice. They are determined by the tilt of the Earth's axis of rotation relative to the planet's orbital plane, and their location varies slowly, predictably and very slightly by about 2.5° latitude over 40,000 years (Gnanadesikan and Stouffer, 2006). In climatology, tropics edges vary seasonally, interannually, and in response to climate forcing. They move poleward in the summer and equatorward in the winter (Davis and Birner, 2013). There are several indicators that define the boundaries of the tropical belt. Generally, three main classes of metrics are employed to estimate the tropical belt borders: circulation-based metrics (e.g., based on the Hadley cells and the subtropical jets), temperature-based metrics (e.g., based on tropopause characteristics), and surface climate metrics (e.g., based on precipitation and surface winds) (Waliser et al., 1999). The common metrics used for TEL determination are discussed in details in (Staten et al., 2018; Adam et al., 2018). TELs estimated applying different metrics not all necessarily yield the same location. Their positions vary by much larger amounts and much more rapidly and unpredictably than the astronomically defined tropics (Lee and Kim, 2003).

Study of tropical belt widening is a challenging task due to the complexity and dynamics of the Earth's atmospheric system and the data limitations. These limitations are the low spatial resolution of RS data as it only covers land and its distribution is not symmetrical in both hemispheres. For the satellite remote sensing technologies and model analyses both suffer from low vertical resolution. Furthermore, reanalyses trends can be biased to reflect changes in both the quality as well as the quantity of the underlying data and the expansion rates computed from different reanalyses were considerably different (Schmidt et al., 2004; Ao and Hajj, 2013). Nowadays, Global navigation satellite systems (GNSS) have provided an exceptional opportunity to retrieve land surface and atmospheric parameters globally (e.g., Jin and Park, 2006; Jin and Zhang, 2016; Wu and Jin, 2014; Jin et al., 2011, 2017), particularly space-borne GNSS Radio Occultation (GNSS-RO) because GNSS-RO has long-term stability and works in all-weather-conditions, which make it a powerful tool for studying climate variability. Since GNSS-RO has uniform global coverage, it covers all locations even at the polar regions and oceans, which are blind zones of other detection systems such as RS and radar. Moreover, GNSS-RO observations

https://doi.org/10.5194/angeo-2021-67
Preprint. Discussion started: 15 December 2021

vertically finer resolved than any of the existing satellite temperature measurements available for the upper-troposphere lower-stratosphere (UTLS) thus GNSS-RO is well suited for this challenge. Moreover, it is a key component for a broad range of other studies, including equatorial waves, Kelvin waves, gravity waves, Rossby and mixed Rossby–gravity waves, and thermal tides (Bai et al., 2020; Scherllin-Pirscher et al., 2021). A number of studies confirmed the feasibility and excellent eligibility of GNSS-RO measurements for monitoring the atmosphere and for climate change detection (Foelsche et al., 2009; Steiner et al., 2011).

Nowadays, GNSS-RO is a valuable remote sounding technique for the atmosphere. During the GNSS-RO event, the GNSS satellite transmit signals that are received onboard a LEO satellite. Due to the atmospheric refractivity, these signals suffer time delay and bending. The atmosphere excess propagation (AEP) is the main observable, and can be calculated with millimeters accuracy, providing high quality and global observations (Wickert et al., 2001a). For instance, the AEP estimate is the base to extract the profiles of bending angle, refractivity, and temperature (Wickert et al., 2004; Xia et al., 2017). The GNSS-RO technique was firstly performed within the US GPS/METeorology experiment for the period from 1995 to 1997 (Kursinski et al., 1997). Also, it is continuously applied aboard various low earth orbiting (LEO) satellite missions since 2001. "These missions are Challenging Mini-satellite Payload (CHAMP) (Wickert et al., 2004; Wickert et al., 2001b); Gravity Recovery and Climate Experiment (GRACE) and Gravity Recovery and Climate Experiment Follow-on (GRACE-FO) (Wickert et al., 2009); Scientific Application Satellite-C/D (SAC-C/D) (Hajj et al., 2004); TerraSAR-X; TanDEM-X; Constellation Observing System for Meteorology, Ionosphere, and Climate (COSMIC/COSMIC-2, also known as FORMOSAT-3/FO RMOSAT-7); the Meteorological Operational satellite Programme-A/B/C (MetOp-A/B/C); FengYun-3C/D (FY-3C/D) (Sun, 2018); Communications/Navigation Outage Forecasting System(C/NOFS); Korea Multi-Purpose Satellite-5 (KOMPSAT-5); the Indian Space Research Organization spacecraft Ocean Satellite-2 (OceanSat-2); and Spanish PAZ (peace in Spanish). A few missions were retired, such as COSMIC-1, GRACE, CHAMP, and SAC-C/D, and some missions are completed by the end of 2020, such as FY-3C, TanDEM-X/TerraSAR-X, KOMPSAT-5, OceanSat-2, and C/NOFS. More missions are planned for the future like MetOp Second Generation (MetOp-SG), FengYun-3E/F/G/H (FY-3E/F/G/H), TerraSAR-X Next Generation (TSX-NG), Jason Continuity of Service-A/B (JASON-CS-A/B", also known as Sentinel 6A/6B), and Meteor-MP N1/N2. By 2025, the planned missions will provide around 14,700 RO profiles daily (Jin et al., 2013; Oscar, 2020)".

In recent years, monitoring the tropopause has received an increased attention for climate change studies. Many studies signified the tropopause rise as a result of the troposphere warming caused by the increase of the GHGs emissions in the atmosphere (Meng et al., 2021; Pisoft et al., 2021). The tropopause characteristics are important for the understanding of the exchange of troposphere-stratosphere (Holton et al., 1995). In addition, the chemical, dynamical, and radiative connections between the troposphere and stratosphere are crucial to understand and predict climate change worldwide. Exchanges of water, mass, and gases between the troposphere and stratosphere occurs through the tropopause. Several studies have investigated the tropopause over the tropics using different data types, and have revealed the problem of the TEL shift (Ao and Hajj, 2013; Tegtmeier et al., 2020; Kedzierski et al., 2020). GNSS-RO provided high accuracy remote sensing

https://doi.org/10.5194/angeo-2021-67
Preprint. Discussion started: 15 December 2021

observations of the thermal structure of the tropopause and was used to investigate the trend and variability of the tropopause (Son et al., 2011). Among the most outstanding advantages of GNSS-RO are their high accuracy of 0.2–0.5 K in estimating temperature in the UTLS region and vertical resolution of 200 m. These advantages make GNSS-RO especially appropriate to detect the possible tropical belt widening based on the height metrics of the tropopause (Kursinski et al., 1997; Ho et al., 2012). Using tropopause metrics for TEL determination have many advantages because they can be accurately estimated from remotely sensed temperature profiles with sufficient vertical resolution, such as GNSS-RO profiles (Davis and Birner, 2013; Seidel and Randel, 2006).

In this study, we investigate the TEL variability from different sources, mainly GNSS-RO data. In Section 2, a description of the GNSS-RO data and other data sets used in our study is presented. In addition, the methods to derive TEL and the data analysis are presented. Section 3 describes and discusses the results of the analysis, and our conclusion and summary are given in Section 4.

2. Data and Methods

2.1. Data

In this study we employ the following data sets:

- The main data used in this study is GNSS-RO atmospheric profiles data from 12 LEO missions from June 2001 to November 2020. The data (CDAAC, 2021) is available at the COSMIC Data Analysis and Archive Center (CDAAC). The GNSS-RO data availability and its time span are shown in Figure 1.

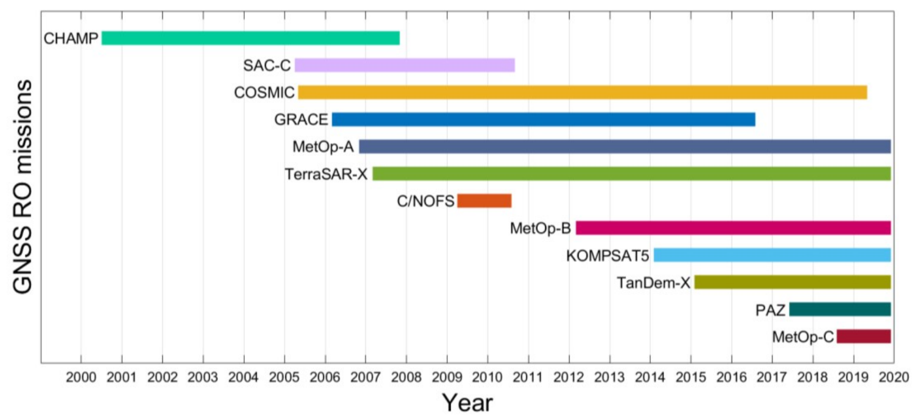

Fig. 1 GNSS-RO data used in this study.

- ERA5 is the fifth generation ECMWF reanalysis for the global climate and weather. Monthly averaged temperature data on pressure levels from ERA5 that provides global coverage for the period from Jun.2001 to Nov.2020 are used to calculate the LRT tropopause height and temperature. The horizontal resolution of the ERA5 data is 0.25° × 0.25°, while the vertical coverage covers from 1000 hPa to 1 hPa, with a vertical resolution of 37 pressure levels (Hersbach et al., 2019a).
- The Atmospheric Infrared Sounder (AIRS) is the spectrometer onboard the second Earth Observing System (EOS) polar-orbiting platform, Aqua. In combination with the

Advanced Microwave Sounding Unit (AMSU), AIRS constitutes an innovative atmospheric sounding instrument with infrared and microwave sensors. LRT height and temperature data provided by AIRS (AIRX3STM v7.0) are provided monthly and have global coverage, with horizontal resolution of 1º × 1º (Aumann et al., 2003; AIRS, 2019a). In this study we use data for the period from September 2002 to November 2020. The data is available at (AIRS, 2019a).

- The Modern-Era Retrospective analysis for Research and Applications version 2 (MERRA-2) provides total column ozone (TCO) at a global scale, monthly, and has a spatial resolution of 0.5° × 0.625°. In this work, we use data from June 2001 to November 2020. The data is to be compared with the LRT height from GNSS-RO. In addition, TCO can provide information about the tropics behavior and can help in emphasizing the GNSS-RO outputs (GMAO, 2015).
- CarbonTracker is a CO_2 measurement and modeling system developed by NOAA Earth System Research Laboratories (ESRL) to keep track of CO_2 sources and sinks throughout the world. Monthly column average CO_2 data with a global coverage from June 2001 to March 2019 is used in this study (Jacobson et al., 2020). The data has spatial resolution of 2° x 3°. Here we use this data to study the behavior and trend of CO_2 which is the most important GHG and the largest forcing component in climate change.
- AIRS provides monthly measurements of CH_4 at 24 pressure levels at a spatial resolution of 1° x 1° (AIRS, 2019b). We employ data from September 2002 to November 2020. CH_4 plays a crucial role in global warming as it is one of the main GHGs that drives long-term climate change.
- Global monthly average surface temperature data from ERA5 reanalysis has horizontal resolution of 0.25° x 0.25° (Hersbach et al., 2019b). In this study we utilize data from June 2001 to November 2020. The purpose of using this data is to study the impacts of the variability in the tropics on the global climatological parameters.
- Monthly average precipitation data is available from the Global Precipitation Climatology Project (GPCP) at horizonal resolution of 2.5° x 2.5° (Adler et al., 2016). We use data from June 2001 to November 2020. The purpose of this data is to investigate the relation between the tropical belt width and the corresponding precipitation pattern.
- Precipitation and Potential Evapotranspiration (PET): Global monthly average precipitation and PET at horizontal resolution of 0.5° x 0.5° are available from the Climatic Research Unit (CRU) Time-Series (TS). This data is employed to compute the SPEI, meteorological drought index. We utilize data from June 2001 to November 2020. The data is available at (Harris et al., 2020). The SPEI drought index was calculated following the indications of (Vicente-Serrano et al., 2010; Beguería et al., 2013).

2.2. Methods

The GNSS-RO temperature profiles with a uniform coverage worldwide have been used to calculate the tropopause height and the tropopause temperature based on both tropopause definitions LRT and CPT. According to the definition of World Meteorological Organization (WMO) "The thermal LRT is defined as the lowest level at which the lapse rate decreases to 2°C/km or less, provided also the average lapse rate between this level and all higher levels within

https://doi.org/10.5194/angeo-2021-67
Preprint. Discussion started: 15 December 2021

2 km does not exceed 2°C/km" (WMO, 1957). While, the CPT is indicated by the minimum temperature in a vertical profile of temperature (Holton et al., 1995). Here, in order to avoid outliers, the tropopause height values of both definitions are limited between 6-20 km. The results of LRT and CPT are subsequently gridded into 5° x 5°. Finally, the spatial and temporal variability of all climatic parameters are investigated using the Principal Component Analysis (PCA) technique (Calabia and Jin, 2016; Calabia and Jin, 2020). This technique provides a new set of modes that provide the variance through a linear combination of the original variables, based on Eigen Decomposition. The solution is a couple of matrices containing the eigenvalues and corresponding eigenvectors of the initial dataset. Each eigenvector is regarded as a map, the eigenvalues provide the percentage of the contribution to the total variability, and the temporal coefficients are used to represent the maps at a given epoch. The first PCA mode has the largest variance, and the following modes represent the next level of variance, which usually are a residual variability. For this reason, since the variability of the variables used in this study are mainly driven by the annual variation, we only employ the first PCA component for each case.

The locations of TEL are estimated from monthly zonal average of LRT height derived from GNSS-RO, ERA5, and AIRS data. The ERA5 and AIRS tropopause parameters are resampled at the same resolution of GNSS-RO. The zonal average LRT height is interpolated as a function of latitude (Ao and Hajj, 2013), and the TEL is determined at each hemisphere using two tropopause height metrics. The first method relies on subjective criterion, according to the first method TEL defined as the latitude at which the LRT height falls 1.5 km under the tropical average (15°S–15°N) LRT height (Davis and Rosenlof, 2012). The second method is an objective criterion, in which the TEL is defined as the latitude of maximum LRT height meridional poleward gradient (Davis and Rosenlof, 2012). Moreover, the rate of expansion and/or contraction of the tropical belt is estimated from both calculation methods, at each hemisphere, independently. In addition, the trend and spatial-temporal variability of CO_2 and CH_4, as important drivers of global warming and as a result tropical widening, are investigated. Furthermore, the trend and spatial-temporal pattern of TCO that give information about the tropical belt width and its patterns of variability is investigated. Finally, we broadly examine the surface temperature, precipitation, and drought trends as meteorological parameters which may have a changing behavior as a response to tropics expansion.

3. Results and Analysis

3.1. Tropopause characteristics from GNSS-RO

Figure 2 shows the GNSS LRT and CPT parameters from June 2001 to November 2020. As shown in Figure 2, the CPT height is always higher than that of LRT. The mean difference between them is about 2.62 km, and there is no significant correlation 0.21. The LRT temperature is higher than that of the CPT. The mean difference between them is about 4.02 k, and the correlation coefficient is 0.4. Our results are consistent with previous studies that displayed a global increase of the tropopause height from radiosonde observations (Seidel and Randel, 2006) and reanalysis (Santer et al., 2004).

https://doi.org/10.5194/angeo-2021-67
Preprint. Discussion started: 15 December 2021

Annales Geophysicae
Discussions

Our analysis shows global increasing trend of LRT height of 36 m/decade since 2001 and this has good agreement with that of Schmidt et al (2008) which shown upward trend of global LRT height of 39–66 m/decade. The LRT temperature show an increase of 0.09 k/decade. For the LRT definition, the correlation coefficient between the LRT height and temperature is -0.78. In case of CPT definition, the global trend of CPT height has increased 60 m/decade since 2001, but that of CPT temperature has decreased 0.09 k/decade. The correlation coefficient between the CPT height and temperature is -0.82.

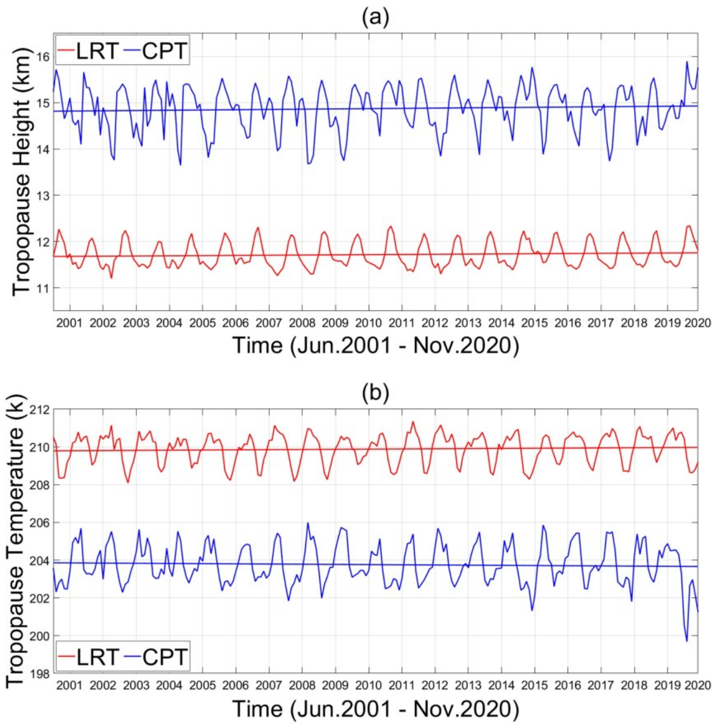

Fig.2 The LRT and CPT (**a**) height and (**b**) temperature is shown from 2001 to 2020.

3.2. Comparison between GNSS, ERA5, and AIRS

In this study, TEL is estimated from the monthly zonal average tropopause height retrieved from the LRT definition. This is done because the LRT represents the location of the point of thermal transition between troposphere and stratosphere. Furthermore, it reacts to both tropospheric and stratospheric temperature changes. Many studies (Seidel and Randel, 2006; Santer et al., 2004) have shown that LRT height is a good indicator of climate change. Figure 3 shows the LRT height values derived from GNSS, ERA5, and AIRS. In general, AIRS shows the highest values of LRT height, while GNSS shows the lowest values. The trends show that ERA5 data has the highest increasing rate of LRT height, being 48 m/decade since June, 2001. In contrast, AIRS has the lowest rates for LRT height, showing an increase of 12 m/decade since September, 2002.

https://doi.org/10.5194/angeo-2021-67
Preprint. Discussion started: 15 December 2021

Annales Geophysicae Discussions
Open Access

The zonal mean of LRT height for the 3 data sets during January, April, July, and October of 2008 are shown in figure 4. In January 2008, the high LRT covered higher latitudes in SH than in the NH. The opposite occurs in July. In April 2008, the high LRT covered similarly in both hemispheres. In October, the area covered with high tropopause at NH is larger than that of SH, but not as wide as the coverage in July. This suggest that the warmer the air the wider the area covered with high tropopause. As stated in section 3, the TEL at NH and SH have been estimated applying 2 tropopause height metrics. The results are discussed in detail in the followings.

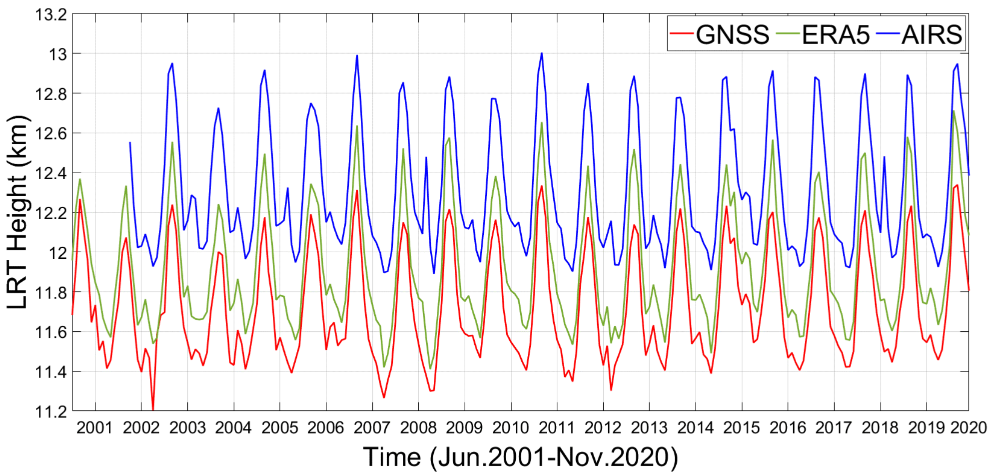

Fig. 3 LRT height from GNSS, ERA5, and AIRS.

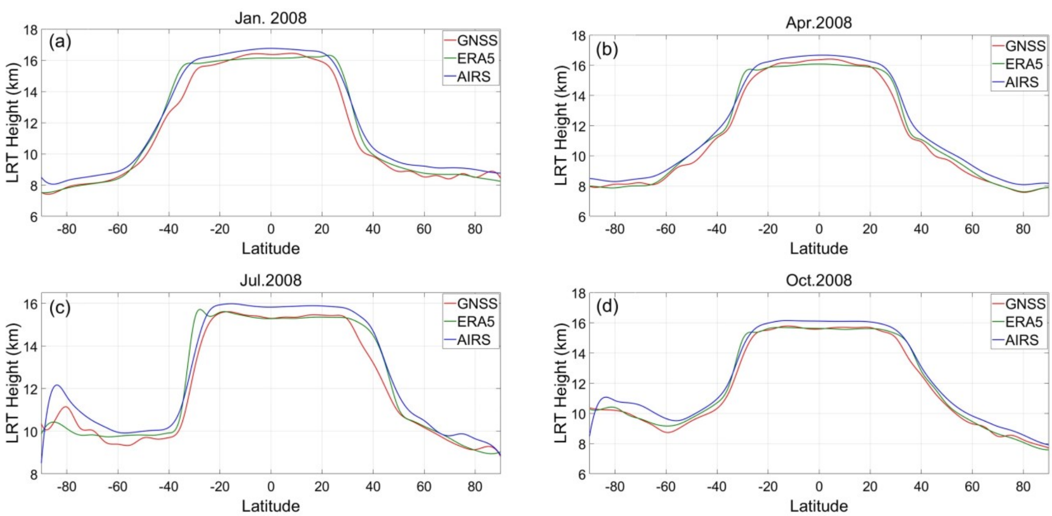

Fig. 4 Monthly zonal average LRT height from GNSS, ERA5 and AIRS.

https://doi.org/10.5194/angeo-2021-67
Preprint. Discussion started: 15 December 2021

3.2.1. Subjective Criterion for TEL

According to subjective criterion (Davis and Rosenlof, 2012), the TEL at each hemisphere is the latitude at which the tropopause height is 1.5 km under the tropical average tropopause height (15°S-15°N). As shown in figure 5 and table 1, the tropical belt based on GNSS has expanded 0.41°/decade in the NH, and 0.08°/decade in the SH, since 2001. Using GNSS-RO data the tropical belt expansion trends in NH and SH agree to some extent with the results of Ao and Hajj (2013). According to Meng et al (2021) the highest trend of LRT height is covering latitudinal band 30°N to 40°N and this possibly caused by the tropical widening and subtropical jet poleward shift over the past four decades (Staten et al., 2018), showing high agreement with our findings. In case of ERA5, there is no significant expansion or contraction at both hemispheres. On the other side, AIRS has expansion of about 0.34°/decade at the NH and strong contraction of about -0.48°/decade at the SH.

Table.1 Tropical belt expansion and contraction rates based on subjective criterion.

Source	Duration	NH		SH	
GNSS	Jun.2001-Nov.2020	0.41	±0.09	0.08	± 0.04
ERA5	Jun.2001-Nov.2020	-0.01	±0.1	-0.04	± 0.05
AIRS	Sep.2002-Nov.2020	0.34	± 0.11	-0.48	±0.05

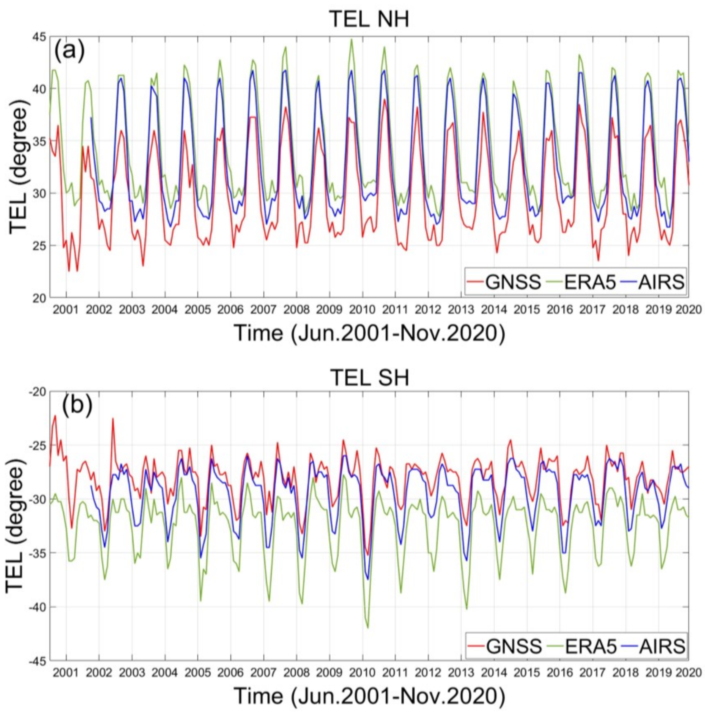

Fig. 5 TEL using subjective criterion for TEL at (**a**) NH and (**b**) SH.

https://doi.org/10.5194/angeo-2021-67
Preprint. Discussion started: 15 December 2021

3.2.2. Objective Criterion for TEL

According to objective criterion (Davis and Rosenlof, 2012), TEL at each hemisphere is the latitude of maximum poleward gradient of tropopause height. As shown in figure 6 and table 2, the tropical belt based on GNSS has expanded about 0.13°/decade in the NH since 2001, but there is no significant expansion or contraction in the SH. In case of ERA5, there is no significant signal in NH, while SH has a minor contraction of approximately -0.08°/decade. On the other side, AIRS capture an expansion of 0.13°/decade in NH, and strong contraction in SH of -0.37°/decade. It is clear from these results, that the rates of expansion and contraction using the objective criterion are less than that of the subjective criterion. For the objective method, TEL occurrences are located more poleward than that of the subjective method.

Table.2 Tropical belt expansion and contraction rates based on objective criterion.

Source	**Duration**	**NH**		**SH**	
GNSS	Jun.2001-Nov.2020	0.13	± 0.1	-0.03	±0.06
ERA5	Jun.2001-Nov.2020	- 0.06	±0.1	- 0.08	± 0.06
AIRS	Sep.2002-Nov.2020	0.13	± 0.04	-0.37	±0.06

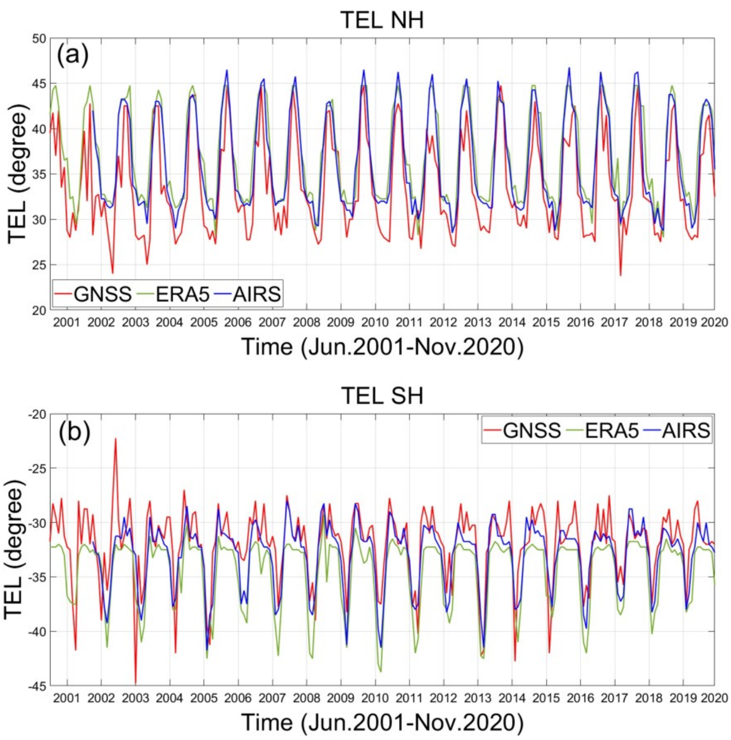

Fig.6 TEL using objective criterion, (**a**) TEL at NH and (**b**) TEL at SH.

https://doi.org/10.5194/angeo-2021-67
Preprint. Discussion started: 15 December 2021

3.3. Spatial and Temporal Variability of LRT

In this section, the LRT height and temperature are investigated between 50°N to 50°S. Figure 7 shows the analyses results for LRT height and temperature. At the NH, the LRT height has increased about 48 m/decade since 2001 and this is consistent with that of Meng et al (2021) which shown increase of LRT height around 44.4 m/decade over 20°N to 80°N for the period from 2001 to 2020. In contrast, LRT height at the SH shows a slight decrease of -2.4 m/decade. Regarding to LRT temperature, it has increased about 0.21 k/decade for NH and 0.34 k/decade for SH. Both hemispheres LRT temperature time series show increasing rates higher than that of the global 0.09 k/decade. Figure 7 also shows the temporal and spatial variability given by the 1st PCA. The temporal variability for LRT Height captures 22.79% of the total variance. For the LRT temperature, PCA1 captures 13.47% of the total variability. These values are relatively small, showing that the variability spreads along lower degree PCA modes. We can clearly see the annual forcing. The spatial variability shows similar patterns for LRT height and temperature. The signal at the NH is stronger and wider than that at the SH.

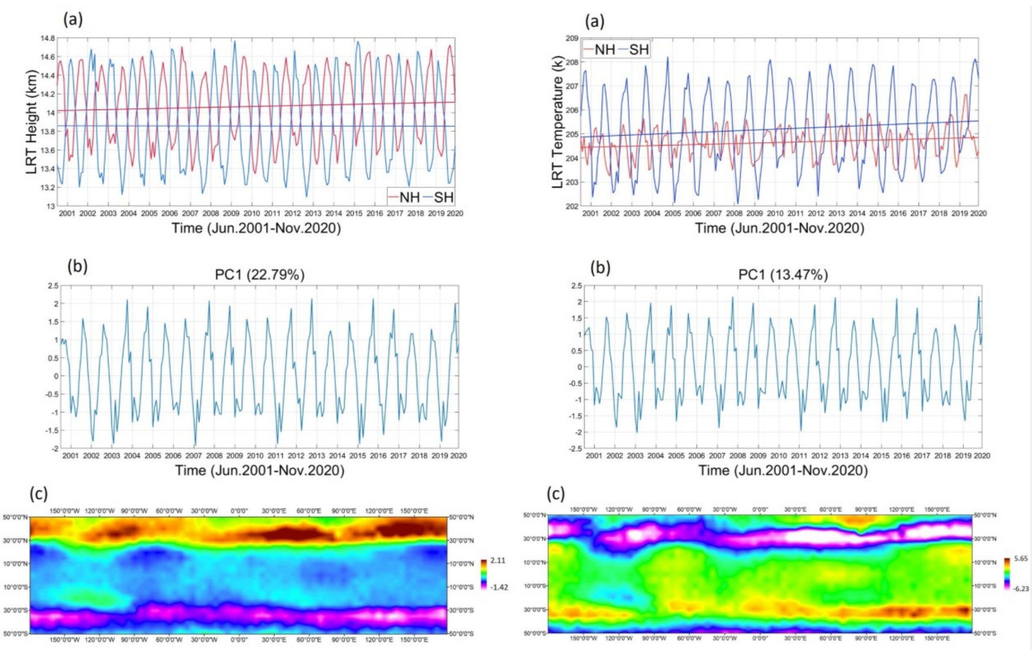

Fig.7 GNSS-RO based LRT height (left) and temperature (right). In (**a**) temporal time series (**b**) temporal variability given by PCA1, and (**c**) spatial variability map given by PCA1.

3.4. Total Column Ozone (TCO), Carbon dioxide (CO_2), and Methane (CH_4)

Figure 8 shows that since 2001, TCO has increased globally 0.7 DU/decade. TCO has a strong correlation of -0.64 with the LRT height. In the NH, the TCO has increased 0.06 DU/decade, while in the SH 1.05 DU/decade. The PCA1 of TCO represents the 66.68% of the total variability. The spatial map of PCA1 shows stronger signal at the NH than that at the SH. The NH signal is located more poleward than that of the SH. Comparisons with GNSS-RO LRT height spatial and temporal

https://doi.org/10.5194/angeo-2021-67
Preprint. Discussion started: 15 December 2021

Annales Geophysicae Discussions Open Access EGU

pattern suggest the TCO expansion at the NH, and a weak expansion or non-significant contraction at the SH.

CO_2 is the most important GHG and it is considered a main driver of global warming. The time series of the CO_2 is shown in figure 8. In this figure, we can see CO_2 increase of 21.38 ppm/decade since 2001. This variable has a correlation of -0.05 with GNSS LRT height. CO_2 column average in both NH and SH has the same increasing rate of 21.6 ppm/decade. This is higher than the global rate. The STD at NH is 11.38 which is higher than that of SH 10.90. The temporal variability given by the PCA1 capture 77.64% of the total variability. PCA1 shows increasing trend and large variability with time. The map of PCA1 variability shows a shift toward the north pole. This seems to be related to the coverage of the tropical belt i.e., the TEL occurrence at the NH is more pole ward than that of the SH.

CH_4 is one of the main GHGs, and it is considered a long-term driver of climate change. The global time series of CH_4 column average (Fig. 8a) shows increasing trend of 39 ppb/decade since 2001. This variable has a correlation of 0.23 with GNSS-RO LRT height. CH_4 column average in both NH and SH show equal increasing trends 46.8 ppb/decade. This is higher than the global rate. The STD at the NH is similar to that of the SH 25.91. The temporal variability PCA1 capture 40.65% of the total variability. PCA1 shows non-significant trend but the range increases with time. The map of PCA1 shows more pole ward signal in the NH than its equivalent at the SH. The NH signal reaches 30°N, and the SH signal does not reach the limit of 30°S. This is clearly in with the TEL results, showing the tropical condition in the NH cover a wider area than that at the SH.

https://doi.org/10.5194/angeo-2021-67
Preprint. Discussion started: 15 December 2021

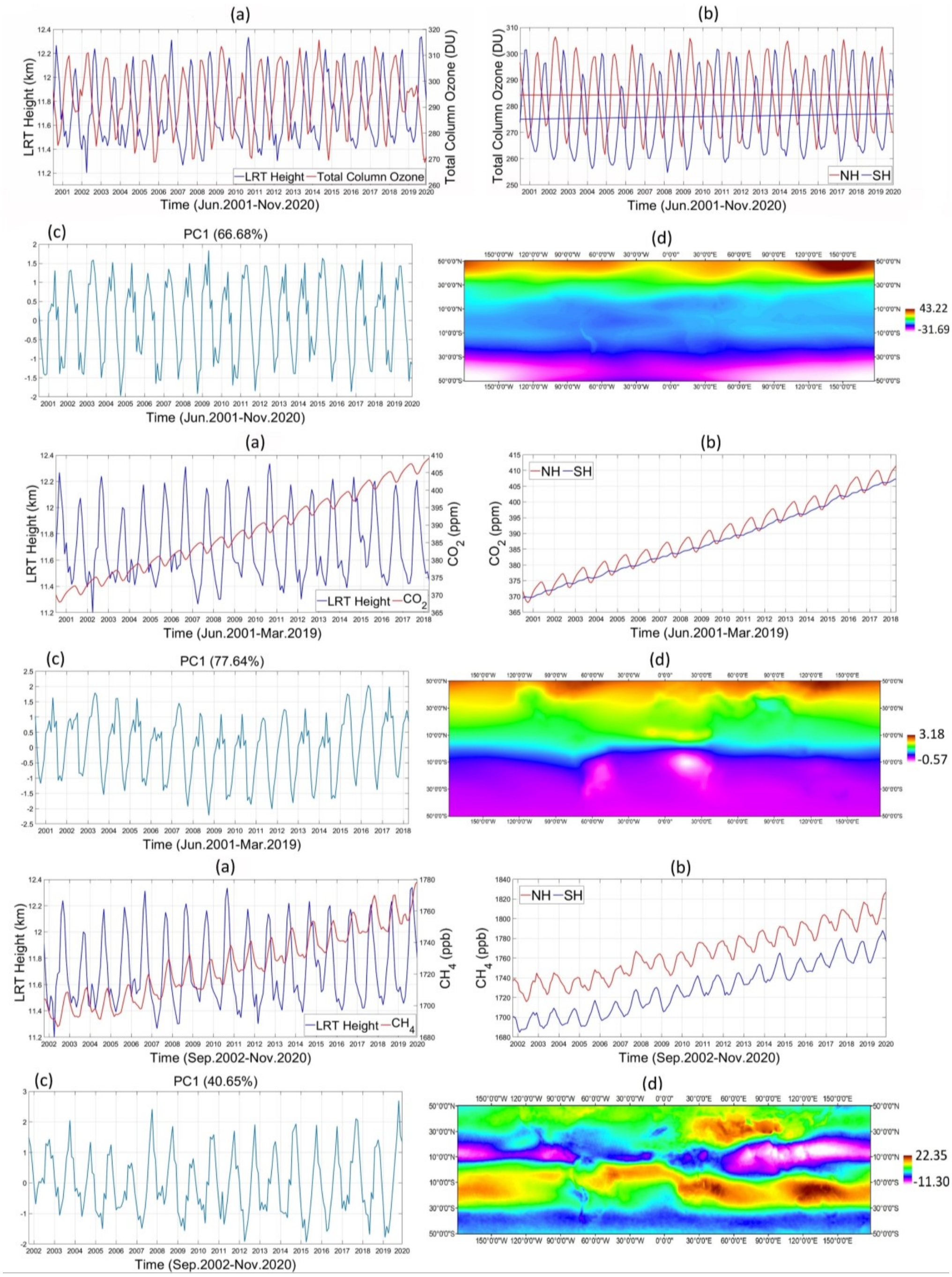

Fig.8 TCO (top), CO_2 (middle), and CH_4 (bottom) results. In (**a**) temporal time series against LRT height (**b**) temporal time series at NH and SH (**c**) temporal variability given by PCA1 and (**d**) spatial variability map given by PCA1.

https://doi.org/10.5194/angeo-2021-67
Preprint. Discussion started: 15 December 2021

3.5. Surface Temperature and GPCP Precipitation

Figure 9 shows the global surface temperature has increased 0.3 k/decade since 2001. A clear correlation between the surface temperature and the GNSS-RO LRT height is seen, with a value of 0.81. The surface temperature in both NH and SH shows an increasing trend of 0.23 k/decade and 0.18 k/decade, respectively. The surface temperature at the NH has STD of 3.5. This value is higher than that of the SH 1.5. The PCA1 capture 84.41% of the total variance. The PCA1 shows an increasing trend and amplitude with time. The PCA1 map has a weaker signal in the SH than that in the NH. The results of surface temperature agree with the GNSS-RO TEL. For instance, the NH show higher expansion than at the SH which shows a minor expansion using subjective criterion and non-significant contraction applying objective criterion. Hence, these results support surface temperature as a proposed driver for tropics expansion (Allen et al., 2012a; Adam et al., 2014).

The GPCP Precipitation show a global decrease of -0.04 mm/decade since 2001. The precipitation behavior has strong correlation of 0.61 with the GNSS LRT height. The GPCP Precipitation in the NH show a minor decreasing trend -0.02 mm/decade meanwhile the SH shows a significant decreasing trend -1.3 mm/decade. The precipitation at the NH has STD of 15.84 and the SH of 16.47. The PCA1 capture 29.30% of the total variability. PCA1 has increasing trend and amplitude with time. The PCA1 map shows a pattern at the north side of the equator.

https://doi.org/10.5194/angeo-2021-67
Preprint. Discussion started: 15 December 2021

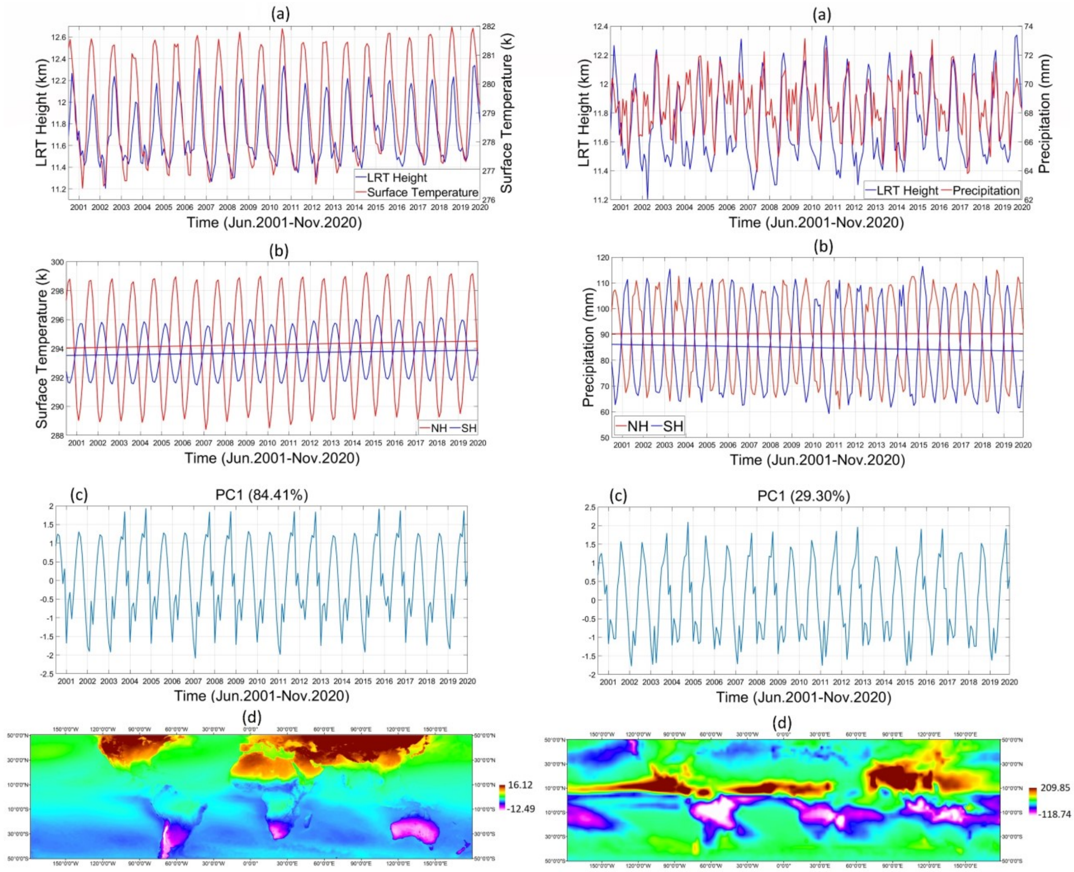

Fig.9 Surface Temperature (left) and GPCP precipitation (right). In (**a**) temporal time series against LRT height (**b**) temporal time series at NH and SH (**c**) temporal variability given by PCA1 and (**d**) spatial variability map given by PCA1.

3.6. Standardized Precipitation Evapotranspiration Index (SPEI)

The SPEI is usually employed to monitor the meteorological drought status. Figure 10 shows the SPEI has increased 0.056 per decade since 2001. The NH show an increase of 0.035 per decade, and the SH decreased -0.005 per decade. This variable has no correlation with GNSS LRT height -0.002. Because the study area is wide and extends through many continents, the SPEI, in our study, only provides information about the dry and wet condition. Figure 10 shows the spatial pattern of SPEI in September 2019, and the areas by category of no-drought, moderate, severe, and extreme. Figure 11 shows the number of cells covered with drought, and its corresponding classification from figure 10. The total number of cells covered with drought at the NH nearly double its value at the SH. Both hemispheres have a decreasing trend of the number of cells covered with drought. The decrease rate is 510 cell/decade at the NH and 373 cell/decade at the SH. The drought does not show any spatial pattern regarding the location of TEL.

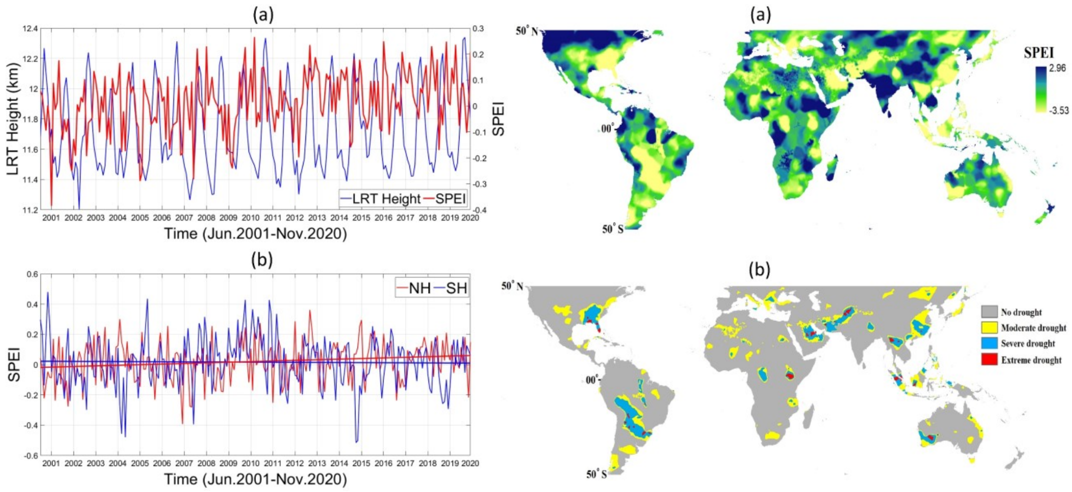

Fig.10 On the left, SPEI drought index (**a**) global SPEI time series in comparison with LRT height and (**b**) SPEI for two latitudinal bands 0°-50°N & 0°-50°S. On the right, (**a**) SPEI drought index in September 2019 and (**b**) SPEI drought categories in September 2019.

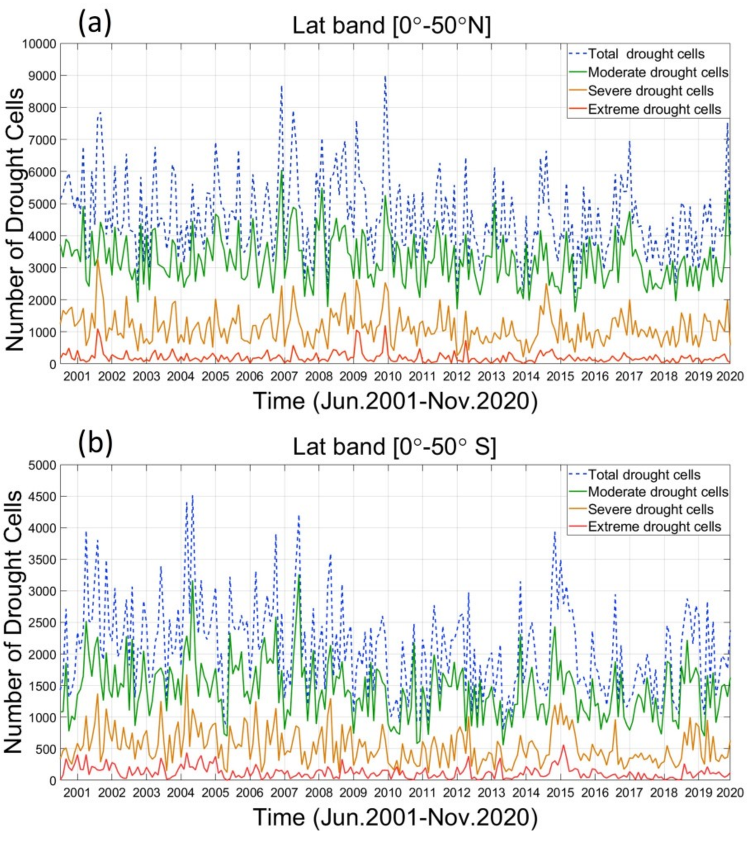

Fig.11 Number of cells covered with drought at (**a**) NH and (**b**) SH.

https://doi.org/10.5194/angeo-2021-67
Preprint. Discussion started: 15 December 2021

4. Conclusions

The GNSS-RO is a well-established technique to derive atmospheric temperature structure in the UTLS region. In this study, GNSS-RO data of 12 RO missions are combined together to examine the possible tropical belt expansion. GNSS-RO profiles are employed to derive tropopause height and temperature based on LRT and CPT definitions. Our analyses show that LRT and CPT height have increased 36 m/decade and 60 m/decade, respectively, since June, 2001. There is high correlation between the tropopause height and temperature, being -0.78 and -0.82 for LRT and CPT, respectively. Comparison with the LRT height from ERA5 shows an increase of 48 m/decade since June, 2001, while that derived from AIRS has a smaller increase 12 m/decade since September, 2002.

TEL at each hemisphere is estimated using two tropopause height metrics. Applying the first method, subjective criterion, there are higher expansion and contraction rates than that from the second method, objective criterion. While using the objective criterion, the locations of TEL at both hemispheres are more poleward than that from the subjective criterion. For the subjective method, tropical width results from GNSS-RO have an expansive behavior in the NH with about 0.41°/decade, and a minor expansion trend in the SH with 0.08°/decade. On the other side, ERA5 has non-significant contraction in both hemispheres. For the AIRS data, there is a clear expansion behavior in the NH with about 0.34°/decade, and a strong contraction in the SH with -0.48°/decade. In case of objective method, GNSS-RO has an expansion behavior in the NH with about 0.13°/decade, but there is no significant expansion or contraction in the SH. Results of several studies, based on different data sets and metrics, shown an expansive behavior of tropical belt in NH higher than that of SH (Hu and Fu, 2007; Archer and Caldeira, 2008; Hu et al., 2010; Zhou et al., 2011; Allen et al., 2012b). This broadly agree with our GNSS-RO based results. For the ERA5, there is no significant signal in the NH, while the SH has a minor contraction of about -0.08°/decade. The AIRS data show an expansion value in the NH with 0.13°/decade, and strong contraction in SH with -0.37°/decade. From all data sets, the TEL is located more poleward in the NH than in the SH. For both subjective and objective methods, the TEL reach the latitudes of 44.75°N and 46.75°N, respectively, at the NH. Meanwhile, at the SH the TEL reach the latitudes of 42°S and 44.75°S for subjective and objective methods, respectively. In both hemispheres, the variability of tropopause parameters (temperature and height) is maximum around the TEL locations.

The TCO shows increasing rates globally. The rate in the SH is higher than that of the NH. The ozone variability agrees well with the spatial and temporal modes of TEL estimated from GNSS-RO LRT height. This supports GNSS-RO TEL estimates over that of ERA5 and AIRS. On the other side, CO_2 and CH_4, as the main GHGs responsible for global warming, show a global increasing rate. Their increasing rate at the NH and the SH are nearly the same. The patterns of TCO and CO2 display good agreement with the TEL locations at NH and SH. They show more poleward occurrence with time and the variability in NH is higher than that of SH. In addition, CH4 has signal at NH occurs more poleward than that at SH. The surface temperature and the precipitation both increase with time, and have strong correlation with LRT height. Both variables show an increasing rate at the NH higher than at the SH. The surface temperature shows strong

https://doi.org/10.5194/angeo-2021-67
Preprint. Discussion started: 15 December 2021

Annales Geophysicae Discussions

spatial variability pattern that broadly agrees with the TEL locations from GNSS-RO. The spatial pattern of precipitation shows northward orientation. The SPEI meteorological drought index shows increasing rate globally, and NH shows increasing trend while SH shows decreasing trend. Since SPEI is multivariate, it has no direct response to the TEL behavior. In both hemispheres, the number of cells covered with drought decreased since 2001. The study results signify the importance of monitoring the tropopause and TEL parameters that can accurately indicate the climate variability and climate change globally.

Funding: This study was supported by the National Natural Science Foundation of China (NSFC) Project (Grant No. 12073012), National Natural Science Foundation of China-German Science Foundation (NSFC-DFG) Project (Grant No. 41761134092), China Scholarship Council (CSC) and Ministry of Higher Education of the Arab Republic of Egypt.

Author contributions

M.D. provided the main ideas, developed the methodology, conceived and performed the experiments, and analyzed the results; S.G. provided supervision, mentorship, and funding support; A.C. provided manuscript edition and revision tasks; A.S. helped in manuscript writing and editing.

Competing interests. The authors declare that they have no conflict of interest.

Acknowledgements

The authors thanks to the CDAAC for providing GNSS-RO data, NOAA ESRL for providing CarbonTracker CT2019B, and Copernicus Climate Change Service Information for MERRA-2 & ERA5 data. We are grateful to the Climate Research Unit (CRU), the University of Delaware (UDEL), and Global Precipitation Climatology Center (GPCC) for granting access to datasets. The first author especially thanks to National Research Institute of Astronomy and Geophysics, Egypt, and to Nanjing University of Information Science and Technology, China, for granting the scholarship for pursuing his Ph.D.

References

Adam, O., Grise, K. M., Staten, P., Simpson, I. R., Davis, S. M., Davis, N. A., Waugh, D. W., Birner, T., and Ming, A.: The TropD software package (v1): standardized methods for calculating tropical-width diagnostics. Geoscientific Model Development, 11(10), 4339–4357. https://doi.org/10.5194/gmd-11-4339-2018, 2018.

Adam, O., Schneider, T., and Harnik, N.: Role of Changes in Mean Temperatures versus Temperature Gradients in the Recent Widening of the Hadley Circulation. Journal of Climate, 27(19), 7450–7461. https://doi.org/10.1, 2014.

Adler, R., Wang, J., Sapiano, M., Huffman, G., Chiu, L., Xie, P., Ferraro, R., Schneider, U., Becker, A., Bolvin, D., Nelkin, E., Gu, G., and NOAA CDR Program.: Global Precipitation Climatology Project (GPCP) Climate Data Record (CDR), Version 2.3 (Monthly). National Centers for Environmental Information. doi:10.7289/V56971M6, 2016.

https://doi.org/10.5194/angeo-2021-67
Preprint. Discussion started: 15 December 2021

Annales Geophysicae Discussions
Open Access

AIRS project: Aqua/AIRS L3 Monthly Standard Physical Retrieval (AIRS-only) 1 degree x 1 degree V7.0, Greenbelt, MD, USA, Goddard Earth Sciences Data and Information Services Center (GES DISC), 10.5067/UBENJB9D3T2H, 2019a.

AIRS project: Aqua/AIRS L3 Monthly Standard Physical Retrieval (AIRS+AMSU) 1 degree x 1 degree V7.0, Greenbelt, MD, USA, Goddard Earth Sciences Data and Information Services Center (GES DISC), 10.5067/KUC55JEVO1SR, 2019b.

Allen, R. J., Sherwood, S. C., Norris, J. R., and Zender, C. S.: The equilibrium response to idealized thermal forcings in a comprehensive GCM: implications for recent tropical expansion. Atmospheric Chemistry and Physics, 12(10), 4795–4816. https://doi.org/10.5194/acp-12-4795-2012, 2012a.

Allen, R. J., Sherwood, S. C., Norris, J. R., and Zender, C. S.: Recent Northern Hemisphere tropical expansion primarily driven by black carbon and tropospheric ozone. Nature, 485(7398), 350–354. https://doi.org/10.1038/nature11097, 2012b.

Ao, C. O., and Hajj, J. A.: Monitoring the width of the tropical belt with GPS radio occultation measurements, Geophys. Res. Lett., 40, 6236–6241, doi: 10.1002/2013GL058203, 2013.

Archer, C. L., and Caldeira, K.: Historical trends in the jet streams. Geophysical Research Letters, 35(8). https://doi.org/10.1029/2008gl033614, 2008.

Aumann, H., Chahine, M., Gautier, C., Goldberg, M., Kalnay, E., McMillin, L., Revercomb, H., Rosenkranz, P., Smith, W., Staelin, D., Strow, L., and Susskind, J.: AIRS/AMSU/HSB on the aqua mission: design, science objectives, data products, and processing systems. IEEE Transactions on Geoscience and Remote Sensing, 41(2), 253–264. https://doi.org/10.1109/tgrs.2002.808356, 2003.

Bai, W., Deng, N., Sun, Y., Du, Q., Xia, J., Wang, X., Meng, X., Zhao, D., Liu, C., Tan, G., Liu, Z., and Liu, X.: Applications of GNSS-RO to Numerical Weather Prediction and Tropical Cyclone Forecast. Atmosphere, 11(11), 1204. https://doi.org/10.3390/atmos11111204, 2020.

Beguería, S., Vicente-Serrano, S. M., Reig, F., and Latorre, B.: Standardized precipitation evapotranspiration index (SPEI) revisited: parameter fitting, evapotranspiration models, tools, datasets and drought monitoring. International Journal of Climatology, 34(10), 3001–3023. https://doi.org/10.1002/joc.3887, 2013.

Calabia, A., and Jin, S.: New Modes and Mechanisms of Long-Term Ionospheric TEC Variations From Global Ionosphere Maps. Journal of Geophysical Research: Space Physics, 125(6). https://doi.org/10.1029/2019ja027703, 2020.

Calabia, A., and Jin, S.: New modes and mechanisms of thermospheric mass density variations from GRACE accelerometers. Journal of Geophysical Research: Space Physics, 121(11), 11,191-11,212. https://doi.org/10.1002/2016ja022594, 2016.

CDAAC: https://cdaac- ww.cosmic.ucar.edu/cdaac /products.html, last access: 20 March 2021.

Davis, N. A., and Birner, T.: Seasonal to multidecadal variability of the width of the tropical belt. Journal of Geophysical Research: Atmospheres, 118(14), 7773–7787. https://doi.org/10.1002/ jgrd.50610, 2013.

Davis, S. M., and Rosenlof, K. H.: A Multidiagnostic Intercomparison of Tropical-Width Time Series Using Reanalyses and Satellite Observations. Journal of Climate, 25(4), 1061–1078. https://doi.org/10.1175/jcli-d-11-00127.1, 2012.

https://doi.org/10.5194/angeo-2021-67
Preprint. Discussion started: 15 December 2021

Annales Geophysicae Discussions
Open Access

Foelsche, U., Pirscher, B., Borsche, M., Kirchengast, G., and Wickert, J.: Assessing the Climate Monitoring Utility of Radio Occultation Data: From CHAMP to FORMOSAT-3/COSMIC. Terrestrial, Atmospheric and Oceanic Sciences, 20(1), 155. https://doi.org/10.3319/tao.2008.01.14.01(f3c), 2009.

GMAO (Global Modeling and Assimilation Office), MERRA-2 instM_2d_asm_Nx: 2d,Monthly mean,Single-Level,Assimilation,Single-Level Diagnostics V5.12.4, Greenbelt, MD, USA, Goddard Earth Sciences Data and Information Services Center (GES DISC), 10.5067/5ESKGQTZG7FO, 2015.

Gnanadesikan, A., and Stouffer, R. J.: Diagnosing atmosphere-ocean general circulation model errors relevant to the terrestrial biosphere using the Köppen climate classification. Geophysical Research Letters, 33(22). https://doi.org/10.1029/2006gl028098, 2006.

Grise, K. M., Davis, S. M., Simpson, I. R., Waugh, D. W., Fu, Q., Allen, R. J., Rosenlof, K. H., Ummenhofer, C. C., Karnauskas, K. B., Maycock, A. C., Quan, X. W., Birner, T., and Staten, P. W.: Recent Tropical Expansion: Natural Variability or Forced Response? Journal of Climate, 32(5), 1551–1571. https://doi.org/10.1175/jcli-d-18-0444.1, 2019.

Hajj, G. A., Ao, C. O., Iijima, B. A., Kuang, D., Kursinski, E. R., Mannucci, A. J., Meehan, T. K., Romans, L. J., de la Torre Juarez, M., and Yunck, T. P.: CHAMP and SAC-C atmospheric occultation results and intercomparisons. Journal of Geophysical Research: Atmospheres, 109(D6), n/a. https://doi.org/10.1029/2003jd003909, 2004.

Harris, I., Osborn, T.J., Jones, P. et al.: Version 4 of the CRU TS monthly high-resolution gridded multivariate climate dataset. Sci Data 7, 109: https://doi.org/10.1038/s41597-020-0453-3, 2020.

Hersbach, H., Bell, B., Berrisford, P., Biavati, G., Horányi, A., Muñoz Sabater, J., Nicolas, J., Peubey, C., Radu, R., Rozum, I., Schepers, D., Simmons, A., Soci, C., Dee, D., Thépaut, J-N.: ERA5 monthly averaged data on pressure levels from 1979 to present. Copernicus Climate Change Service (C3S) Climate Data Store (CDS). 10.24381/cds.6860a573, 2019a.

Hersbach, H., Bell, B., Berrisford, P., Biavati, G., Horányi, A., Muñoz Sabater, J., Nicolas, J., Peubey, C., Radu, R., Rozum, I., Schepers, D., Simmons, A., Soci, C., Dee, D., Thépaut, J-N.: ERA5 monthly averaged data on single levels from 1979 to present. Copernicus Climate Change Service (C3S) Climate Data Store (CDS). 10.24381/cds.f17050d7, 2019b.

Ho, S. P., Hunt, D., Steiner, A. K., Mannucci, A. J., Kirchengast, G., Gleisner, H., Heise, S., von Engeln, A., Marquardt, C., Sokolovskiy, S., Schreiner, W., Scherllin-Pirscher, B., Ao, C., Wickert, J., Syndergaard, S., Lauritsen, K. B., Leroy, S., Kursinski, E. R., Kuo, Y. H., Gorbunov, M.: Reproducibility of GPS radio occultation data for climate monitoring: Profile-to-profile inter-comparison of CHAMP climate records 2002 to 2008 from six data centers. Journal of Geophysical Research: Atmospheres, 117(D18), n/a. https://doi.org/10.1029/2012jd017665, 2012.

Holton, J. R., Haynes, P. H., McIntyre, M. E., Douglass, A. R., Rood, R. B., and Pfister, L.: Stratosphere-troposphere exchange, Rev. Geophys., 33(4), 403-439, doi:10.1029/95RG02097, 1995.

Hu, Y., and Fu, Q.: Observed poleward expansion of the Hadley circulation since 1979. Atmospheric Chemistry and Physics, 7(19), 5229–5236. https://doi.org/10.5194/acp-7-5229-2007, 2007.

Hu, Y., Zhou, C., and Liu, J.: Observational evidence for poleward expansion of the Hadley circulation. Advances in Atmospheric Sciences, 28(1), 33–44. https://doi.org/10.1007/s00376-010-0032-1, 2010.

https://doi.org/10.5194/angeo-2021-67
Preprint. Discussion started: 15 December 2021

Annales Geophysicae Discussions

Jacobson, A. R., Schuldt, K. N., Miller, J. B., Oda, T., Tans, P., Arlyn Andrews, Mund, J., Ott, L., Collatz, G. J., Aalto, T., Afshar, S., Aikin, K., Aoki, S., Apadula, F., Baier, B., Bergamaschi, P., Beyersdorf, A., Biraud, S. C., Bollenbacher, A., … Miroslaw Zimnoch.: CarbonTracker CT2019B. NOAA Global Monitoring Laboratory. https://doi.org/10.25925/20201008, 2020.

Jin, S.G., and Park, P.: Strain accumulation in South Korea inferred from GPS measurements, Earth Planets Space, 58(5), 529-534, doi: 10.1186/BF03351950, 2006.

Jin, S.G., Han, L., and Cho, J.: Lower atmospheric anomalies following the 2008 Wenchuan Earthquake observed by GPS measurements. J. Atmos. Sol.-Terr. Phys., 73(7-8), 810-814, doi: 10.1016/j.jastp.2011.01.023, 2011.

Jin, S., Cardellach, E., and Xie, F.: GNSS Remote Sensing: Theory, Methods and Applications (Remote Sensing and Digital Image Processing, 19) (2014th ed.). Springer, 2013.

Jin, S.G., and Zhang, T.: Terrestrial water storage anomalies associated with drought in Southwestern USA derived from GPS observations. Surv. Geophys., 37(6), 1139-1156, doi: 10.1007/s10712-016-9385-z, 2016.

Jin, S.G., Jin,R., and Kutoglu, H.: Positive and negative ionospheric responses to the March 2015 geomagnetic storm from BDS observations. J. Geodesy, 91(6), 613-626, doi: 10.1007/s00190-016-0988-4, 2017.

Kedzierski, R., Matthes, K., and Bumke, K.: New insights into Rossby wave packet properties in the extratropical UTLS using GNSS radio occultations. 10.5194/acp-2020-124, 2020.

Kursinski, E. R., Hajj, A. G., Hardy, R. K., Schofield, T. J., and Linfield, R.: Observing the Earth's atmosphere with radio occultation measurements using the Global Positioning System, J. Geophys. Res., 102, 23,429–23,465, doi: 10.1029/97JD01569, 1997.

Lee, S., and Kim, H.: The Dynamical Relationship between Subtropical and Eddy-Driven Jets. Journal of the Atmospheric Sciences, 60, 1490-1503, 2003.

Meng, L., Liu, J., Tarasick, D. W., Randel, W. J., Steiner, A. K., Wilhelmsen, H., Wang, L., and Haimberger, L.: Continuous rise of the tropopause in the Northern Hemisphere over 1980–2020. Science Advances, 7(45). https://doi.org/10.1126/sciadv.abi8065, 2021.

Oscar: https://www.wmo-sat.info/oscar/gapanalyses?mission=9, last accessed on 15 August 2020.

Pisoft, P., Sacha, P., Polvani, L. M., Añel, J. A., de la Torre, L., Eichinger, R., Foelsche, U., Huszar, P., Jacobi, C., Karlicky, J., Kuchar, A., Miksovsky, J., Zak, M., and Rieder, H. E.: Stratospheric contraction caused by increasing greenhouse gases. Environmental Research Letters, 16(6), 064038. https://doi.org/10.1088/1748-9326/abfe2b, 2021.

Santer, B. D., Wigley, T. M. L., Simmons, A. J., Kållberg, P. W., Kelly, G. A., Uppala, S. M., Ammann, C., Boyle, J. S., Brüggemann, W., Doutriaux, C., Fiorino, M., Mears, C., Meehl, G. A., Sausen, R., Taylor, K. E., Washington, W. M., Wehner, M. F., and Wentz, F. J.: Identification of anthropogenic climate change using a second-generation reanalysis. Journal of Geophysical Research: Atmospheres, 109(D21), n/a. https://doi.org/10.1029/2004jd005075, 2004.

Scherllin-Pirscher, B., Steiner, A. K., Anthes, R. A., Alexander, M. J., Alexander, S. P., Biondi, R., Birner, T., Kim, J., Randel, W. J., Son, S. W., Tsuda, T., and Zeng, Z.: Tropical Temperature Variability in the

https://doi.org/10.5194/angeo-2021-67
Preprint. Discussion started: 15 December 2021

UTLS: New Insights from GPS Radio Occultation Observations. Journal of Climate, 34(8), 2813–2838. https://doi.org/10.1175/jcli-d-20-0385.1, 2021.

Schmidt, T., Wickert, J., Beyerle, G., and Heise, S.: Global tropopause height trends estimated from GPS radio occultation data. Geophysical Research Letters, 35(11). https://doi.org/10.1029/2008gl034012, 2008.

Schmidt, T., Wickert, J., Beyerle, G., and Reigber, C.: Tropical tropopause parameters derived from GPS radio occultation measurements with CHAMP. Journal of Geophysical Research: Atmospheres, 109(D13), n/a. https://doi.org/10.1029/2004jd004566, 2004.

Seidel, D. J., and Randel, W. J.: Variability and trends in the global tropopause estimated from radiosonde data. Journal of Geophysical Research, 111(D21). https://doi.org/10.1029/2006jd007363, 2006.

Son, S. W., Tandon, N. F., and Polvani, L. M.: The fine-scale structure of the global tropopause derived from COSMIC GPS radio occultation measurements. Journal of Geophysical Research, 116(D20). https://doi.org/10.1029/2011jd016030, 2011.

Staten, P. W., Lu, J., Grise, K. M., Davis, S. M., and Birner, T.: Re-examining tropical expansion. Nature Climate Change, 8(9), 768–775. https://doi.org/10.1038/s41558-018-0246-2, 2018.

Steiner, A. K., Lackner, B. C., Ladstädter, F., Scherllin-Pirscher, B., Foelsche, U., and Kirchengast, G.: GPS radio occultation for climate monitoring and change detection. Radio Science, 46(6). https://doi.org/10.1029/2010rs004614, 2011.

Tegtmeier, S., Anstey, J., Davis, S., Dragani, R., Harada, Y., Ivanciu, L., Kedzierski, R., Krüger, K., Legras, B., Long, C., Wang, J., Wargan, K., and Wright, J.: Temperature and tropopause characteristics from reanalyses data in the tropical tropopause layer. Atmospheric Chemistry and Physics. 20. 753-770. 10.5194/acp-20-753-2020, 2020.

Vicente-Serrano, S. M., Beguería, S., and López-Moreno, J. I.: A Multiscalar Drought Index Sensitive to Global Warming: The Standardized Precipitation Evapotranspiration Index. Journal of Climate, 23(7), 1696–1718. https://doi.org/10.1175/2009jcli2909.1, 2010.

Waliser, D. E., Shi, Z., Lanzante, J. R., and Oort, A. H.: The Hadley circulation: assessing NCEP/NCAR reanalysis and sparse in-situ estimates. Climate Dynamics, 15(10), 719–735. https://doi.org/10.1007/s003820050312, 1999.

Watt-Meyer, O., Frierson, D. M. W., and Fu, Q.: Hemispheric Asymmetry of Tropical Expansion Under CO_2 Forcing. Geophysical Research Letters, 46(15), 9231–9240. https://doi.org/10.1029/2019gl083695, 2019,

Wickert, J., Galas, R., Beyerle, G., König, R., and Reigber, C.: GPS ground station data for CHAMP radio occultation measurements. Physics and Chemistry of the Earth, Part A: Solid Earth and Geodesy, 26(6–8), 503–511. https://doi.org/10.1016/s1464-1895(01)00092-8, 2001a.

Wickert, J., Michalak, G., Schmidt, T., Beyerle, G., Cheng, C. Z., Healy, S. B., Heise, S., Huang, C. Y., Jakowski, N., Köhler, W., Mayer, C., Offiler, D., Ozawa, E., Pavelyev, A. G., Rothacher, M., Tapley, B., and Köhler, C.: GPS Radio Occultation: Results from CHAMP, GRACE and FORMOSAT-3/COSMIC. Terrestrial, Atmospheric and Oceanic Sciences, 20(1), 35. https://doi.org/10.3319/tao.2007.12.26.01(f3c), 2009.

https://doi.org/10.5194/angeo-2021-67
Preprint. Discussion started: 15 December 2021

Wickert, J., Reigber, C., Beyerle, G., König, R., Marquardt, C., Schmidt, T., Grunwaldt, L., Galas, R., Meehan, T. K., Melbourne, W. G., and Hocke, K.: Atmosphere sounding by GPS radio occultation: First results from CHAMP. Geophysical Research Letters, 28(17), 3263–3266. https://doi.org/10.1029/2001gl013117, 2001b.

Wickert, J., Schmidt, T., Beyerle, G., König, R., Reigber, C., and Jakowski, N.: The Radio Occultation Experiment aboard CHAMP: Operational Data Analysis and Validation of Vertical Atmospheric Profiles. Journal of the Meteorological Society of Japan. Ser. II, 82(1B), 381–395. https://doi.org/10.2151/jmsj.2004.381, 2004.

WMO: Meteorology—A three dimensional science: Second session of the commission for aerology. Geneva: World Meteorological Organization (WMO). (WMO Bull. No. 4), 1957.

Wu, X. R., and Jin, S.G.: GNSS-Reflectometry: Forest canopies polarization scattering properties and modeling, Adv. Space Res., 54(5), 863-870, doi: 10.1016/j.asr.2014.02.007, 2014.

Xia, P., Ye, S., Jiang, K., and Chen, D.: Estimation and evaluation of COSMIC radio occultation excess phase using undifferenced measurements. Atmospheric Measurement Techniques, 10(5), 1813–1821. https://doi.org/10.5194/amt-10-1813-2017, 2017.

Zhou, Y. P., Xu, K. M., Sud, Y. C., and Betts, A. K.: Recent trends of the tropical hydrological cycle inferred from Global Precipitation Climatology Project and International Satellite Cloud Climatology Project data. Journal of Geophysical Research, 116(D9). https://doi.org/10.1029/2010jd015197, 2011.